European Journal of Ophthalmology / Vol. 18 no. 6, 2008 / pp. 915-921

Artificial neural network-based glaucoma diagnosis using retinal nerve fiber layer analysis

D.S. GREWAL[1,2], R. JAIN[1], S.P.S. GREWAL[1], V. RIHANI[3]

[1]Grewal Eye Institute, Chandigarh
[2]Bascom Palmer Eye Institute, Department of Ophthalmology, University of Miami Miller School of Medicine, Palm Beach Gardens, FL - USA
[3]Department of Electronics and Electrical Communication Engineering, Punjab Engineering College, Chandigarh - India

PURPOSE. *To develop, train, and test an artificial neural network (ANN) for differentiating among normal subjects, primary open angle glaucoma (POAG) suspects, and persons with POAG in Asian-Indian eyes using inputs from clinical parameters, optical coherence tomography (OCT), visual fields, and GDx nerve fiber analyzer.*
METHODS. *One hundred eyes were classified using optic disc examination and perimetry into normal (n=35), POAG suspects (n=30), and POAG (n=35). EasyNN-plus simulator was used to develop an ANN model with inputs including age, sex, myopia, intraocular pressure (IOP), optic nerve head, and retinal nerve fiber layer (RNFL) parameters on OCT, Octopus 30-2 full threshold visual field, and GDx parameters.*
RESULTS. *With two outputs (POAG or normal), specificity was 80% and sensitivity was 93.3%. Ninety percent of POAG suspects were labeled as abnormal in this analysis. ANN assigned the highest importance to Smax/Imax RNFL on OCT followed by cup-area (OCT) and other RNFL parameters (OCT) for two outputs. With three outputs (normal, POAG, and POAG suspect), ANN gave an overall classification rate of 65%, specificity of 60%, and sensitivity of 71.4% with a target error rate of the training set at 1%. The parameters for three outputs, in decreasing order of relative importance, were Savg, vertical cup-disc ratio, cup-volume, and cup-area on OCT.*
CONCLUSIONS. *An ANN taking varied diagnostic imaging inputs was able to separate POAG eyes from normal subjects and POAG suspects. The network had reasonable sensitivity with three outputs; however, it had a tendency to mislabel POAG suspects as POAG. (Eur J Ophthalmol 2008; 18: 915-21)*

KEY WORDS. *Artificial neural network, Primary open angle glaucoma, Optical coherence tomography, GDx Variable Corneal Compensation*

Accepted: May 14, 2008

INTRODUCTION

Glaucoma is an optic neuropathy characterized by a gradual loss of retinal ganglion cells and thinning of the retinal nerve fiber layer (RNFL) (1). By 2010, glaucoma is estimated to affect approximately 61 million persons, with 8.4 million suffering from bilateral glaucoma blindness (2). Since glaucomatous optic nerve damage (3) is often asymptomatic in the early stages and leads to irreversible loss of vision, early diagnosis of glaucoma and early detection of glaucoma progression are important because progression can be slowed or halted with appropriate interventions (4).

Clinical examination and grading of fundus photography have been recognized to have limitations in objective assessment of glaucomatous damage due to the wide degree of normal anatomic variation and their subjective nature. Assessment of RNFL thickness and optic nerve head (ONH) topographies by clinical evaluation is subject to disagreement even between experienced observers (5).

Presented in part at the American Society of Cataract and Refractive Surgeons Annual Meeting, San Francisco, CA, 2007 and the World Glaucoma Congress, Singapore, 2007

1120-6721/915-07$25.00/0

Alteration in the structural appearance of the ONH and RNFL usually precedes the development of reproducible glaucomatous visual field defects. Identification of these changes is important in the diagnosis and treatment of glaucoma at early to moderate stages (6). Optical imaging techniques like GDx (7) and optical coherence tomography (OCT) (8) provide an objective and quantitative assessment of optic disc topography and peripapillary RNFL thickness which helps to identify patients at risk for developing visual field defects allowing for early detection of glaucoma (3). The ability to detect glaucoma using these instruments has been described and discussed previously (9, 10).

Artificial neural networks (ANN), like multilayer perceptrons (MLP) with back-propagated learning, trained on RNFL parameters have been used to classify eyes as glaucomatous or healthy (11, 12). Using this method, the neural network classifier is trained to detect a relationship between multiple input parameters and a predefined gold-standard diagnosis by comparing its prediction with the labeled diagnosis and learning from its mistakes. The success of neural network classification methods is most often measured by reporting areas under the receiver operating characteristic curve (AUROC) or by reporting sensitivity at different specificities.

ANNs have been reported to be able to differentiate between glaucoma and normal visual field status at least as well as trained readers (13) and often better than global visual field indices (14, 15). ANNs are superior because they can adapt to the distribution of data rather than assume a predefined distribution (16).

Since OCT provides numerous stereometric measurements of the disc, macula, and peripapillary RNFL, it is important to find the parameters that best allow for the detection of glaucoma. Similarly it has been shown that a combination of multiple parameters with GDx can improve the sensitivity and specificity of discriminating between glaucomatous and healthy eyes (17, 18). Trained classifiers can also be used to predict the diagnosis of new cases (12). Combining the information generated from each instrument can theoretically have a better diagnostic capability.

The purpose of the current study was to develop an automated classifier for discriminating among eyes with primary open angle glaucoma (POAG), normal subjects, and POAG suspects in a South-Asian:Indian population using clinical information and data from the Stratus OCT, GDx-VCC, and visual fields.

METHODS

Subjects

The study was approved by the Institutional Review Board, and adhered to the tenets of the Declaration of Helsinki. Informed consent was obtained from all participants. Healthy subjects, POAG patients, and POAG suspects meeting eligibility criteria described further were enrolled.

Glaucomatous eyes

Eyes were defined as glaucomatous if there was both glaucomatous optic neuropathy (GON) and glaucomatous VF loss. GON was defined as intereye cup-disc ratio asymmetry >0.2, accounting for disc size; rim thinning or notching; peripapillary hemorrhages; or cup-disc ratio greater than or equal to 0.6. Glaucomatous VF loss was diagnosed if any of the following findings were present: 1) three adjacent points depressed by 5 dB, with one of the points depressed by at least 10 dB; 2) two adjacent points depressed by 10 dB; or 3) a 10-dB difference across the nasal horizontal meridian in two adjacent points. None of the points could be edge points unless immediately above or below the nasal horizontal meridian. Thirty-five eyes of 35 such patients were included.

Glaucoma suspects

A glaucoma suspect was defined as a person with an intraocular pressure (IOP) greater than or equal to 22 mm Hg, measured with Goldman Applanation Tonometry (GAT) between 10 AM and 12 PM, on more than two visits without treatment and with visual field results not meeting the above criteria for damage.

Glaucoma patients and glaucoma suspects recruited had undergone one previous threshold VF prior to this study. Thirty eyes of 30 subjects who were classified as POAG suspects were included.

Healthy eyes

Normal controls were recruited among spouses, visitors, and staff of the clinic. Controls had no personal or family history of glaucoma, had an IOP less than or equal to 21 mmHg (measured with GAT between 10 AM and 12 PM), did not use any IOP-lowering medications, had a normal

VF not meeting the criteria for glaucomatous VF loss, and had a normal optic nerve. Thirty-five eyes of 35 normal subjects were included.

All participants (normal subjects, subjects with glaucoma, and glaucoma suspects) had best-corrected visual acuity of 20/40 or better and refractive error between –6.00 and +6.00 diopters (spherical equivalent). Subjects were excluded if they exhibited signs of retinal or ONH pathologies other than glaucoma or if media opacity or a poorly dilating pupil interfered with clinical viewing or imaging of the fundus. Patients were also excluded if they had systemic diseases which could affect the retina or visual fields (VF) or if they had any previous surgery in the study eye other than an uneventful cataract extraction. Patients with diabetes and hypertension were excluded only if they had ocular changes corresponding to diabetes or hypertension evidenced on fundus examination or with OCT changes. The patient's age, gender, presence of diabetes and/or hypertension, and steroid use were recorded.

Eligible subjects underwent a complete ophthalmic evaluation, including review of medical history, undilated and dilated slit-lamp examination, manifest refraction, central corneal pachymetry, IOP (between 10 AM and 12 PM), gonioscopy, full-threshold 30–2 perimetry (Octopus 1-2-3 perimeter [Interzeag AG, Schlieren, Switzerland]), OCT scanning of disc, macula, and peripapillary RNFL, and GDx Imaging. VF, GDx, and OCT were all performed within a maximum period of 2 weeks. If the tests were conducted on the same day, VF were performed first. Pupils were not pharmacologically dilated during these tests. The technician who performed the testing was masked to the diagnosis of the subject.

Exclusion criteria

Patients who had other intraocular or neurologic disease that affected the RNFL or optic disc, a secondary cause of raised IOP, or significant media opacity were excluded. Eyes with consistently unreliable visual field results (defined as false positives and negatives >33%) were also excluded from the study. The VF results were considered reproducible if the same type, location, and index of abnormality were evident in two consecutive VF tests.

OCT scanning

All OCT scans were performed using Stratus OCT with software version 4.0.1 (Carl Zeiss Meditec) with an axial resolution of ≤10 µm and transverse resolution of 20 µm. OCT protocol in our study included peripapillary RNFL scans done with a fast protocol consisting of three separate circumpapillary circular scans with a diameter of 3.4 mm centered on the optic disc, each of which consisted of 512 A-scans obtained in 1.28 seconds. The results were obtained from the mean of three scans. Circular diagrams showed quadrant (temporal, superior, nasal, and inferior) thickness and clock-hour RNFL thickness. The RNFL thickness was the average thickness along the entire circumference of the optic disc. Fifteen RNFL parameters were used: Imax/Smax, Smax/Imax, Smax/Tavg, Imax/Tavg, Smax/Navg, Max-Min, Smax, Imax, Savg, Iavg, temporal thickness, superior thickness, nasal thickness, inferior thickness, and average thickness.

ONH scans were obtained using the fast ONH radial scan protocol which acquired six 4-mm radial scans in 1.92 seconds to measure optic disc topography. The software automatically determined the edge of the ONH as the end of the retinal pigment epithelium–choriocapillaris. Ten ONH parameters were measured: vertical integrated rim area, horizontal integrated rim width, disc area, cup area, rim area, cup-disc area ratio, horizontal cup-disc ratio, vertical cup-disc ratio, cup area (topographic), and cup volume (topographic).

From the macular scan, we used retinal thickness in nine sectors as well as macular volume. Quality assessment of Stratus OCT scans was determined by an experienced examiner. Only good-quality scans, defined as having a focused ocular fundus images, signal strength greater than 6, and a centered circular ring around the optic disc, were included. ONH images were excluded when the machine incorrectly determined the edge of the ONH as the end of the retinal pigment epithelium–choriocapillaris in the automatic mode; if the ONH image was unacceptable; and when images could not be analyzed such as those with very small cup-disc ratios. RNFL thickness and ONH parameters provided a total of 25 OCT input parameters.

GDx VCC scanning

The GDx Variable Corneal Compensation (VCC) (Carl Zeiss Meditech, San Diego, CA) is a scanning laser polarimeter (SLP) with an integrated polarization modulator developed to quantify the thickness of peripapillary RNFL. It is based on the assumption that the parallel ar-

rangement of microtubules within the RNFL causes a change in the state of polarization of an illuminating laser beam (retardation), which can be measured in the light reflected from the retina (19). The measuring beam of the scanning laser polarimeter, a polarization-modulated laser beam (wavelength, 780 nm), is focused on the retina and it penetrates the birefringent nerve fiber layer. Owing to the birefringent nature of the ocular structures, there is a variation in the propagation velocity of one of the two components of light which consequently results in a signal delay that is measured by a detector. This delay is proportional to the RNFL thickness after compensating for delay produced by the cornea and lens. During the measurement, the polarization effects of the anterior segment are canceled by a corneal polarization compensator. The retardation of the light double-passing the RNFL is proportional to its thickness and is measured at 256 by 256 positions within a field of view of 15 by 15 degrees. RNFL thickness is determined along a 3.2-mm-diameter 8-pixel-wide calculation circle, centered on the disc. Three images from each eye were captured and the image with the highest quality score was used. Six parameters were used from the GDx VCC printout: temporal superior nasal inferior temporal (TSNIT) parameters–TSNIT average, superior average, inferior average, TSNIT standard deviation, inter-eye symmetry, and nerve fiber index.

Neural network

An MLP with back propagation learning based ANN for glaucoma detection was trained and tested using EasyNN-plus (v 6.0) simulator (Neural Planner Software, Cheshire, England). The architecture was a universal feed-forward network with the input layer and output layer of nodes separated by one or more hidden layers of nodes. The hidden layers acted as an intermediary between the input and output layers, extracting useful information obtained during learning. The input layer had 114 nodes which included data for age, sex, myopia, steroid administration, history of diabetes or systemic hypertension, IOP, Octopus 30-2 full threshold program (global visual field indices, mean defect, loss variance, and corrected loss variance) ONH parameters, RNFL and macular thickness on OCT, and GDx parameters. The classification model was cross validated using 20 eyes (normal=5; POAG suspects=8; POAG=7). The model had an output layer (the diagnosis: POAG, POAG suspect, or normal), and three hidden layers with 22, 16, and 9 nodes respectively that extracted useful information during learning and assigned weighted coefficients to components of the input layer. The output was compared with the target output (POAG, POAG suspect, or normal). An error signal was then back propagated and the connection weights adjusted correspondingly. During training, the network constructed a multidimensional space, defined by activation of the hidden nodes. The MLP was tested with two different output modes: a binary output mode—glaucoma or normal, and a mode with three outputs—glaucoma, suspect, or normal.

Receiver operating characteristic curves for the different input parameters were constructed and AUROC values were used to assess the ability to differentiate among normal, POAG and POAG suspect eyes. An area under the ROC curve of 1.0 indicated perfect discrimination while an area of 0.5 indicated no discrimination.

RESULTS

The mean age was 55.9±10.2 years in the normal group, 52.1±11.4 years in the glaucoma group, and 57.4±6.8 years for the POAG suspect group. There was no significant difference in age, central corneal thickness measurements, or refraction status among the three groups ($p>0.05$). The visual field mean deviation for the normal group was –0.8±0.4 dB, the glaucoma group was –3.1±1.7 dB, and for the POAG suspect group was –1.2±0.3 dB. There was a significant difference between normal and glaucoma groups ($p<0.0001$) and between POAG suspect and glaucoma groups ($p=0.002$) but not between normal and POAG suspect groups. The clinical characteristics of the study population, visual field global indices, and the imaging parameters that had significant AUROC values are presented in Table I.

The ANN was tested using two output scenarios: two or three outputs.

Two outputs: Labeled eyes as POAG or normal

The highest ranked parameters using this classification were Smax/Imax RNFL on OCT, cup area (OCT), and other RNFL parameters on OCT. With two outputs (glaucoma or normal), the specificity of the ANN was 80% and the sensitivity was 93.3%. In this analysis it labeled 90% POAG suspects as abnormal.

Three outputs: Labeled eyes as POAG, POAG suspect, or normal

The highest ranked parameters using this classification were Savg (OCT), vertical cup disc ratio (OCT), cup volume (OCT), and cup area (OCT).

With three outputs (POAG, POAG suspect, or normal), the ANN gave an overall classification rate of 65%, specificity of 60%, and a sensitivity of 71.4% with a 1% target error rate of the training set.

The AUROC was the highest for Imax (maximum inferior quadrant thickness) (0.773) (Fig. 1) followed by Smax (maximum superior quadrant thickness) (0.716) (Fig. 2), Smax/Imax (0.703) (Fig. 3), and cup area (0.662) (Fig. 4). Clinical parameters including CCT (AUROC=0.554) and IOP (AUROC=0.545) did not demonstrate a significant discriminating value. None of the global visual field indices had a significant AUROC value.

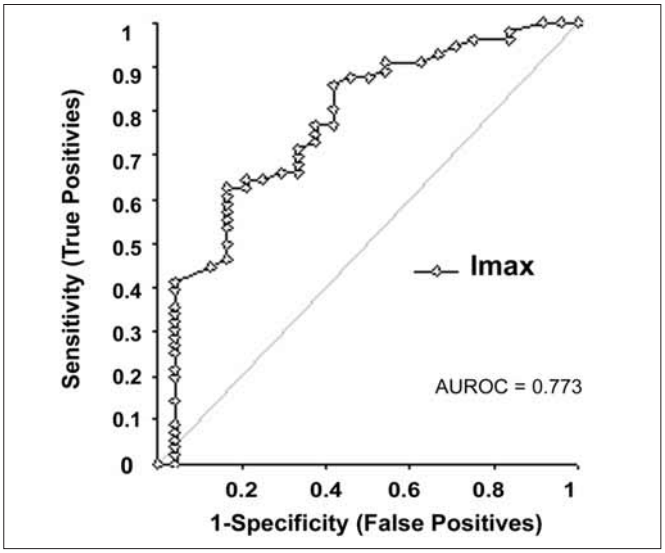

Fig. 1 - *Receiver operating characteristic curve for maximum inferior quadrant thickness (Imax) on optical coherence tomography.*

TABLE I - CHARACTERISTICS OF THE STUDY POPULATION (N=100)

	Normal (n=35)	Suspect (n=30)	Glaucoma (n=35)
Age, years	55.9±10.2	57.4±6.8	52.1±11.4
Gender			
Male	18	13	16
Female	17	17	19
Visual field mean defect	0.8±0.4	1.2±0.3	4.1±1.7
Visual field loss variance	3.25±1.1	3.56±0.9	16.16±8.5
OCT parameters			
Smax/Imax	0.75±0.23	0.84±0.22	1.13±0.26
Imax/Smax	1.12±0.22	1.19±0.15	0.85±0.22
Smax RNFL	128±19	122±17	77±11
Imax	135±22	128±23	85±21
Savg	98±12	94±14	58±16
Iavg	128±22	108±19	64±18
Temporal	80±12	78±12	68±15
Nasal	60±15	59±12	37±15
Average RNFL (µm)	95.9±13.3	91.6±12.2	72.3±14.3
Superior RNFL (µm)	115.3±21.8	112.7±17.2	84.8±22.6
Inferior RNFL (µm)	123.5±17.7	115.9±15.4	88.3±29.9
Cup area (mm^2)	0.44±0.12	0.54±0.15	0.75±0.25
Vertical cup disc ratio (OCT)	0.47±15	0.52±12	0.69±0.12
Cup volume	0.051±0.04	0.059±0.08	0.066±0.12
GDx-VCC parameters (µm)			
TSNIT average	51.2±5.1	50.2±4.4	43.4±6.7
Superior average	61.4±7.2	58.5±6.6	49.62±8.5
Inferior average	63.5±8.2	62.5±6.9	52.6±9.9

Values represent mean ± SD.
OCT = optical coherence tomography; RNFL = retinal nerve fiber layer; GDx-VCC= GDx Variable Corneal Compensation

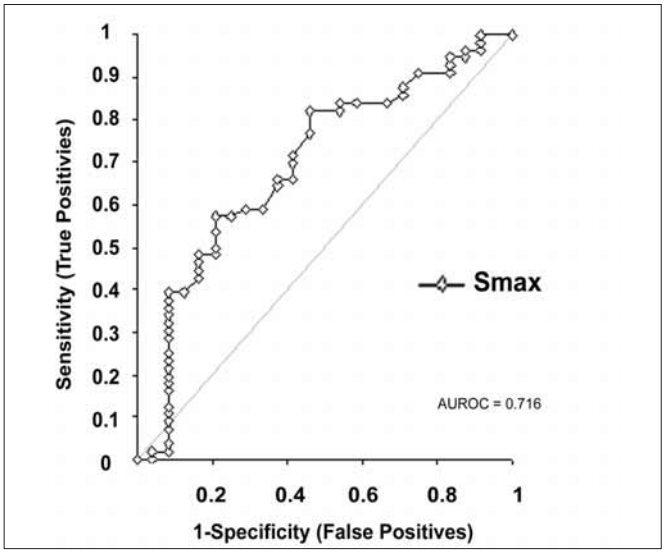

Fig. 2 - *Receiver operating characteristic curve for maximum superior quadrant thickness (Smax) on optical coherence tomography.*

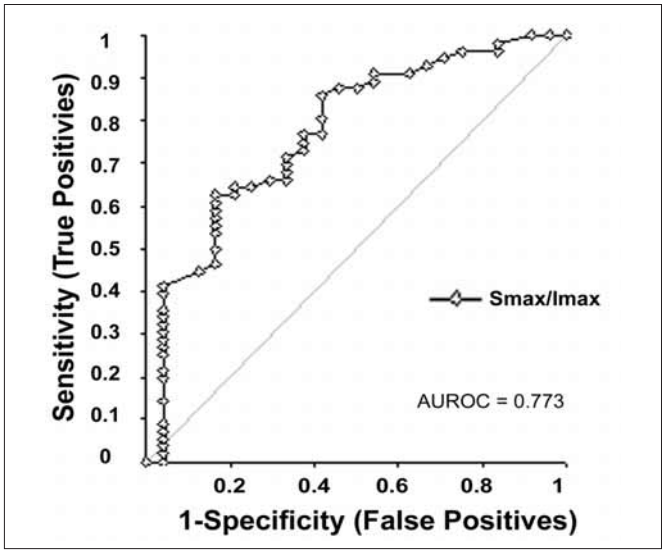

Fig. 3 - *Receiver operating characteristic curve for ratio of maximum superior to maximum inferior quadrant thickness (Smax/Imax) on optical coherence tomography.*

DISCUSSION

An ANN classification model, using data inputs from perimetry, GDx, and OCT were able to separate glaucomatous from normal eyes with a high degree of accuracy. The accuracy however dropped when the outputs were increased to include POAG suspects and the network had a tendency to mislabel POAG suspects as POAG. We believe this could be due to the limited number of input parameters used as the ANN was not able to accurately differentiate patients with varying stages of damage in the glaucoma continuum.

The Smax/Imax RNFL on OCT had the highest sensitivity when using two outputs and the Savg (OCT) had the highest sensitivity when using three outputs. Previous studies have shown Imax to have the highest AUROC among OCT parameters. The AUROC for Imax was almost comparable to that computed in previous studies by Medeiros et al (0.92) (20), Huang and Chen (0.832) (21), and Manassakorn et al (0.92) (22).

In conclusion, we showed that using a combination of RNFL measures obtained using GDx and OCT improved the ability to differentiate between normal eyes, POAG eyes, and POAG suspects. ANNs have been previously shown to perform better than any isolated OCT parameter in distinguishing glaucomatous from normal eyes (23). However, a significant limitation of this study is that local visual field indices were not considered in the ANN.

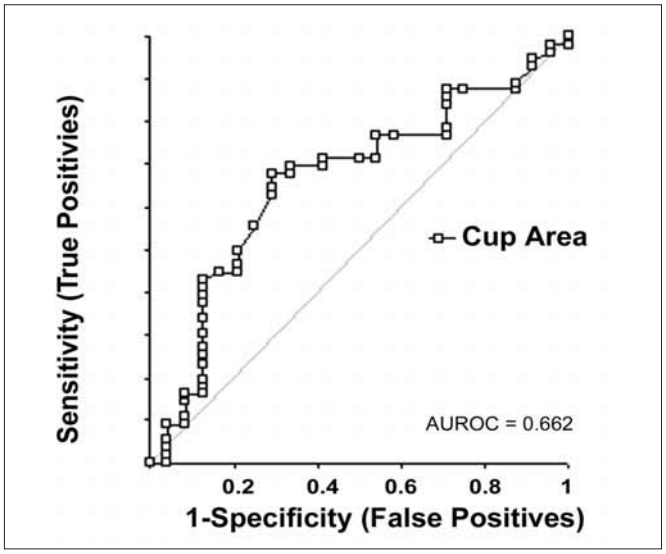

Fig. 4 - *Receiver operating characteristic curve for cup area on optical coherence tomography.*

CONCLUSIONS

ANNs in clinical practice can provide an unbiased classification for diagnosing patients with glaucoma, as glaucoma suspects, or as normal and reduce human-based evaluator bias. Using a combination of input parameters from different imaging modalities could allow a more accurate diagnosis (24).

The clinical acumen of an experienced glaucoma specialist remains the gold standard. A long-term prospective study with additional structural measurements like spectral domain OCT and functional measurements including local visual field indices and other sensitive perimetric tests would be needed to determine the utility of this grading index in discriminating between various types of glaucoma and possibly in evaluating glaucoma progression.

None of the authors has any financial or proprietary interest in this manuscript or received financial support.

Reprint requests to:
Dilraj Grewal, MD
Grewal Eye Institute
SCO 166-169
Sector 9-C
Chandigarh, India 160009
Dilraj@gmail.com

REFERENCES

1. Harwerth RS, Carter-Dawson L, Shen F, et al. Ganglion cell losses underlying visual field defects from experimental glaucoma. Invest Ophthalmol Vis Sci 1999; 40: 2242-50.
2. Quigley HA, Broman AT. The number of people with glaucoma worldwide in 2010 and 2020. Br J Ophthalmol 2006; 90: 262-7.
3. Sommer A, Katz J, Quigley HA, et al. Clinically detectable nerve fiber atrophy precedes the onset of glaucomatous field loss. Arch Ophthalmol 1991; 109: 77-83.
4. Heijl A, Leske MC, Bengtsson B, et al. Reduction of intraocular pressure and glaucoma progression: results from the Early Manifest Glaucoma Trial. Arch Ophthalmol 2002; 120: 1268-79.
5. Varma R, Steinmann WC, Scott IU. Expert agreement in evaluating the optic disc for glaucoma. Ophthalmology 1992; 99: 215-21.
6. Greany MJ, Hoffman DC, Garway-Heath DF, et al. Comparisons of optic nerve imaging methods to distinguish normal eyes from those with glaucoma. Invest Ophthalmol Vis Sci 2002; 43: 140-5.
7. Wollstein G, Garway-Heath DF, Hitchings RA. Identification of early glaucoma cases with the scanning laser ophthalmoscope. Ophthalmology 1998; 105: 1557–63.
8. Sanchez-Galeana C, Bowd C, Blumenthal EZ, et al. Using optical imaging summary data to detect glaucoma. Ophthalmology 2001; 108: 1812-18.
9. Weinreb RN, Shakiba S, Sample PA, et al. Association between quantitative nerve fiber layer measurement and visual field loss in glaucoma. Am J Ophthalmol 1995; 120: 732-8.
10. Hoh ST, Greenfield DS, Mistlberger A, et al. Optical coherence tomography and scanning laser polarimetry in normal, ocular hypertensive, and glaucomatous eyes. Am J Ophthalmol 2000; 129: 129-35.
11. Brigatti L, Hoffman D, Caprioli J. Neural networks to identify glaucoma with structural and functional measurements. Am J Ophthalmol 1996; 121: 511-21.
12. Burgansky-Eliash Z, Wollstein G, Chu T, et al. Optical coherence tomography machine learning classifiers for glaucoma detection: a preliminary study. Invest Ophthalmol Vis Sci 2005; 46: 4147-52.
13. Goldbaum MH, Sample PA, White H, et al. Interpretation of automated perimetry for glaucoma by neural network. Invest Ophthalmol Vis Sci 1994; 35: 3362-73.
14. Lietman T, Eng J, Katz J, Quigley HA. Neural networks for visual field analysis: how do they compare with other algorithms? J Glaucoma 1999; 8: 77-80.
15. Goldbaum MH, Sample PA, Chan K, et al. Comparing machine learning classifiers for diagnosing glaucoma from standard automated perimetry. Invest Ophthalmol Vis Sci 2002; 43: 162-9.
16. Bizios D, Heijl A, Bengtsson B. Trained artificial neural network for glaucoma diagnosis using visual field data: a comparison with conventional algorithms. J Glaucoma 2007; 16: 20-8.
17. Colen TP, Tang NE, Mulder PG, Lemij HG. Sensitivity and specificity of new GDx parameters. J Glaucoma 2004; 13: 28-33.
18. Lauande-Pimentel R, Carvalho RA, Oliveiar HC, et al. Discrimination between normal and glaucomatous eyes with visual field and scanning laser polarimetry measurements. Br J Ophthalmol 2001; 85: 586-91.
19. Niessen AG, Van Den Berg TJ, Langerhorst CT, Greve EL. Retinal nerve fiber layer assessment by scanning laser polarimetry and standardized photography. Am J Ophthalmol 1996; 121: 484-93.
20. Medeiros FA, Zangwill LM, Bowd C, et al. Comparison of the GDx VCC scanning laser polarimeter, HRT II confocal scanning laser ophthalmoscope, and Stratus OCT optical coherence tomography for the detection of glaucoma. Arch Ophthalmol 2004; 122: 827-37.
21. Huang ML, Chen HY. Development and comparison of automated classifiers for glaucoma diagnosis using Stratus optical coherence tomography. Invest Ophthalmol Vis Sci 2005; 46: 4121-9.
22. Manassakorn A, Nouri-Mahdavi K, Caprioli J. Comparison of retinal nerve fiber layer thickness and optic disk algorithms with optical coherence tomography to detect glaucoma. Am J Ophthalmol 2006; 141: 105-15.
23. Huang M, Chen H. Development and comparison of automated classifiers for glaucoma diagnosis using Stratus optical coherence tomography. Invest Ophthalmol Vis Sci 2005; 46: 4121-9.
24. Uchida H, Brigatti L, Caprioli J. Detection of structural damage from glaucoma with confocal laser image analysis. Invest Ophthalmol Vis Sci 1996; 37: 2393-401.